Spin-flip effects in the magnetoluminescence and magnetoresistance of semimagnetic narrow-gap $Hg_{1-x-y}Cd_xMn_yTe$

W. Hoerstel, W. Kraak, and W. T. Masselink*
Humboldt-Universität zu Berlin, Department of Physics, Invalidenstrasse 110, D-10115 Berlin, Germany

Yu. I. Mazur, G. G. Tarasov, and E. V. Kuzmenko
Institute of Semiconductor Physics, National Academy of Sciences, Prospect Nauki 45, 252650 Kiev, Ukraine

J. W. Tomm
Max-Born-Institut für Nichtlineare Optik und Kurzzeitspektroskopie (MBI), Rudower Chaussee 6, D-12489 Berlin, Germany
(Received 15 December 1997; revised manuscript received 6 April 1998)

We report optical and magnetotransport properties in semimagnetic $Hg_{1-x-y}Cd_xMn_yTe$, a narrow-gap semiconductor with an energy gap of about 120 meV. Equivalent phenomena in both optical and magnetotransport measurements of the same set of samples independently indicate selection rules due to the magnetic ions; the photoluminescence (PL) contains optical transitions forbidden by symmetry, and in the longitudinal magnetoresistance a ''last'' H_0^b peak forbidden by the conventional selection rules is observed. At $T=5$ K, the PL feature related to band-to-band-like transitions shows a well-pronounced splitting in both the Faraday and Voigt geometries, with a subsequent decrease of the higher-energy component for $B \geqslant 2$ T, a behavior which substantially differs from that known for ''nonmagnetic'' $Hg_{1-x}Cd_xTe$ with a corresponding energy gap. This fundamental difference can be explained in terms of spin relaxation, found to be strongly different for the above-mentioned materials. The results of PL and Shubnikov–de Haas (SdH) measurements are consistently interpreted in terms of a modified Pidgeon-Brown model which includes the *s-d* exchange interaction between the spin of free carriers and the localized magnetic moments of the Mn^{2+} ions. The exchange parameters are determined both from the PL and SdH data. Spin-flip transitions caused by exchange coupling is assumed to be responsible for the violation of the particular selection rules. [S0163-1829(98)02232-2]

I. INTRODUCTION

A number of recent experimental studies of narrow-gap $Hg_{1-x-y}Cd_xMn_yTe$ have demonstrated that the crystalline structure and band structure, as well as the kinetic parameters of the carriers, are strongly influenced by the presence of magnetic ions, even for small concentrations of typically $y < 0.01$. Such influences are observed in far-infrared reflection and transmission,[1,2] magnetoluminescence,[3] and transport effects.[4] Despite the quaternary composition, the vibrational states in $Hg_{1-x-y}Cd_xMn_yTe$ become less broadened compared with those in ternary $Hg_{1-x}Cd_xTe$ with the same energy gap (E_g).[1] Photoluminescence (PL) from $Hg_{1-x-y}Cd_xMn_yTe$ typically reveals features of an excitonic nature,[3] an unexpected finding for narrow-gap semiconductors, and particularly surprising in a quaternary narrow-gap system.[2] Also, the low-temperature electron mobility in this case was found to be as good as that of $Hg_{1-x}Cd_xTe$ with the same band gap. These strong indications of a significant improvement in several semiconductor characteristics assumed to be related to spin doping (magnetic ions) provides a strong motivation for further study of the exchange interaction between spins of the free carriers and the localized spin moments embedded in a crystalline matrix. For small concentrations of magnetic ions, the intermediate exchange interaction between the localized spin moments is negligible due to the small overlap of the electronic wave functions of neighboring Mn^{2+} ions. Nevertheless, this interaction can become enhanced by the free charge-carrier exchange. The exchange interaction results in a number of spin-dependent phenomena, e.g., the spin splitting of the Landau levels becomes strongly dependent on temperature, and the amplitude of the Shubnikov–de Haas (SdH) oscillations also becomes nonmonotonically dependent on temperature. Exchange interaction can also be invoked to explain a number of other phenomena observed in the magneto-PL and magnetoresistance.

In this study we describe and explain peculiarities in magnetic spin-doped $Hg_{1-x-y}Cd_xMn_yTe$ samples through two independent experiments carried out on the same samples. Both SdH and magneto-PL data are successfully interpreted, taking into account the possibility of spin-flip transitions caused by the influence of *s-d* exchange interaction as well as *p*-type wave-function admixing into the conduction-band states.

II. EXPERIMENTAL DETAILS

$Hg_{0.769}Cd_{0.224}Mn_{0.007}Te$ single crystals were grown by the traveling heater technique. The as-grown *n*-type crystals have been prepared by subsequent cooling at a well-defined low cooling rate. The carrier concentration *n* and the electron mobility μ are typically $(1-3)\times 10^{15}$ cm^{-3} and $(3-5)\times 10^5$ cm^2 V^{-1} s^{-1} at 4.2 K, respectively. The crystal diameter was about 8 mm, and the thickness of the sliced wafers was about 0.3–0.5 mm. The homogeneity of the element distributions was checked by means of x-ray microanalysis,

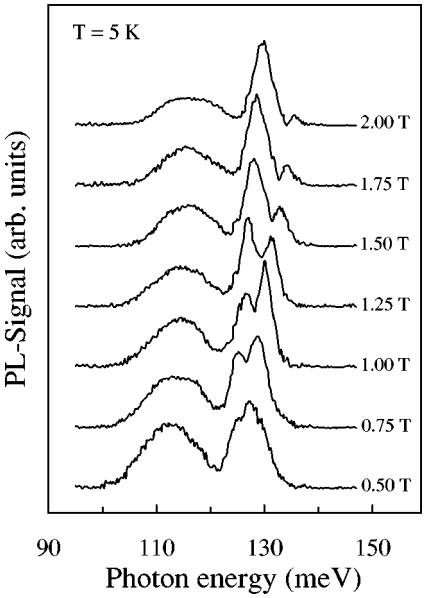

FIG. 1. Low-temperature PL spectra from single-crystalline $Hg_{0.769}Cd_{0.224}Mn_{0.007}Te$ at different magnetic fields in the Voigt geometry.

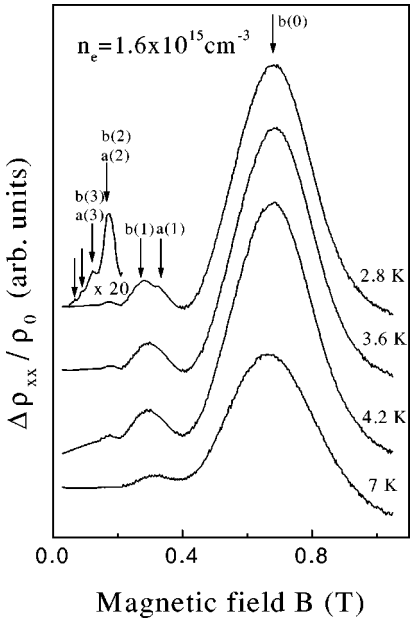

FIG. 2. Temperature dependence of the SdH oscillations in $Hg_{0.769}Cd_{0.224}Mn_{0.007}Te$ (transverse magnetoresistance ρ_{xx}). The low-field part is magnified by a factor 20.

and indicated that, over the entire wafer, the element distributions were constant within the accuracy limits of the method, about $\Delta x = \Delta y = 0.002$. Before the optical measurements, the surfaces were etched in standard Br-methanol solution.

The PL investigations were carried out with a Bruker IFS-88 Fourier transform spectrometer. The signal was excited with a laser emitting at 1.58 eV, and the excitation densities were below 1 W cm^{-2}. Phase-locked excitation and PL detection were realized using a double-modulation technique. An Oxford Spectromag 4000 cryosystem allowed measurement in the 1.4–70-K range at magnetic fields (B) up to $B = 7$ T. Both Voigt and Faraday measuring geometries were investigated.

The transverse (ρ_{xx}) and longitudinal (ρ_{zz}) magnetoresistances were measured in the temperature range 1.5–30 K. Magnetic fields of up to 7 T were applied. The samples used for SdH measurements were the same as used for the optical experiments. They were sliced into rectangular Hall bars with dimensions of $9 \times 1.5 \times 1.2$ mm^3. Ohmic contacts were obtained by soldering with 10% tin-indium.

III. RESULTS AND DISCUSSION

A. Experimental results

Figure 1 depicts typical low-temperature magneto-PL spectra. The main change in the PL spectrum takes place in the magnetic-field region of 0.5–2.0 T. It can be seen that the high-energy PL feature splits into two components followed by a subsequent decrease of the high-energy line for $B \geqslant 2$ T. With increasing magnetic field, the lower-energy line becomes narrower and moves toward higher energies. The very broad low-energy PL feature in the 105–120-meV range is assumed to be impurity related.

The SdH data are presented in Fig. 2. The features of the $\rho_{xx}(B)$ dependence can be assigned according to the selection rules for the SdH oscillations.[5] For the transverse magnetoresistance both the a (spin up) and b (spin down) set (i.e., H_N^a and H_N^b) should appear for each Landau number $N \geqslant 1$. The last peak observed for ρ_{xx} at high magnetic field should, however, be related to H_0^b only. Figure 2 shows the transformation of the SdH pattern with increasing temperature. So, at $T = 2.8$ K, one can distinctly see more than six peaks, among them the most pronounced are the spin-split H_1^b and H_1^a peaks and that of H_0^b . At higher temperatures, the low-field peaks become smeared and at $T = 10$ K only the H_0^b peak is observed. It shifts with increasing temperature toward weaker magnetic fields. For analyzing these features, a Pidgeon-Brown treatment including exchange interaction will be employed.

B. Theory

Here we present a synopsis of the theoretical basis for this work. The Pidgeon-Brown model[6] assumes that the electrons in a magnetic field can be described in the effective-mass approximation, which includes only the Γ_6 (conduction band), Γ_8 (valence band), and Γ_7 (split-off band) interactions, while the contribution of remote bands is taken into account as perturbation up to terms of k^2. Additionally the band electrons interact with the Mn^{2+} ions. In the mean-field approximation, where the electrons are allowed to ''feel'' all the localized magnetic moments in an average way, the interaction is expressed by[7]

$$H_{ex} = y\sigma_z \langle S_z \rangle \sum_{\vec{R}} J(\vec{r} - \vec{R}), \tag{1}$$

where σ_z and S_z are the z projections of the $\hat{\sigma}$ and the $\hat{S}$ spin operators of the band electrons and the magnetic ions, respectively. J is the exchange-interaction constant, the vectors $\vec{r}$ and $\vec{R}$ define the coordinates of the band electrons and of the Mn^{2+} ions, respectively, and $H \| z$. For the zinc-blende

symmetry, the set of basis functions is typically constructed from the S, X, Y, and Z Luttinger-Kohn states. In this basis, the $3d$ orbital singlet of the magnetic ions produces two exchange parameters: $\alpha=\langle S|J|S\rangle$ and $\beta=\langle X|J|X\rangle$. For S_z the thermal average is taken. For the very low manganese content, $y\approx 0.014$, it has been shown[8] that the intersite magnetic interaction of Mn^{2+} ions is negligible, and the thermal average of S_z follows the Brillouin law[9]

$$\langle S_z\rangle = -S_0 B(\tau), \tag{2}$$

where $S_0=\frac{5}{2}$ is the saturation spin value for the localized magnetic moments of the Mn^{2+} ion, and

$$B(\tau)=\frac{2S+1}{2S}\coth\left(\frac{2S+1}{2S}\tau\right)-\frac{1}{2S}\coth\left(\frac{\tau}{2S}\right), \tag{3}$$

$$\tau=\frac{g_{\mathrm{Mn}}\mu_B SH}{k_B T}.$$

Here μ_B is the Bohr magneton, $S=\frac{5}{2}$, and g_{Mn} is the gyromagnetic factor of the Mn^{2+} ions. With increasing manganese content, the probability of Mn ion cluster formation and of antiferromagnetic interactions between the localized magnetic moments become important. In order to take these effects into account empirically, S_0 in Eq. (2) is treated as a fitting parameter, and T in Eq. (3) is replaced by $T_{\mathrm{eff}}=T+T_0$, with T_0 also being an empirical fitting parameter. These parameters directly govern the magnetization of the crystal.

The nonzero matrix elements α and β are incorporated into the 8×8 Pidgeon-Brown matrix, and define the Landau-level positions. In order to determine the energy dispersion, which is necessary for the further treatment, the $\vec{k}\cdot\vec{p}$ approximation matrix is used [cf., e.g., Eq. (11) of Ref. 10],

$$D=\begin{bmatrix} D_a & D_c \\ D_c^+ & D_b \end{bmatrix}, \tag{4}$$

with the 4×4 matrices D_a and D_b determining the a (spin-up) and b (spin-down) sets of Landau levels, respectively. The D_c matrix elements explicitly include the k dependence, and will be used for the calculation of the transition probability between the Landau levels,

$$D_c=\begin{bmatrix} 0 & 0 & D_{13} & D_{14} \\ 0 & 0 & D_{23} & D_{24} \\ D_{13}^* & D_{23}^* & 0 & D_{34} \\ D_{14}^* & D_{24}^* & D_{34}^* & 0 \end{bmatrix}, \tag{5}$$

where $D_{13}=\sqrt{2/3}Pk_z$, $D_{14}=i\sqrt{1/3}Pk_z$, $D_{23}=i\sqrt{2}\varsigma k_z k^-$, $D_{24}=-\varsigma k_z k^+$, $D_{34}=\sqrt{3}\varsigma k^+$, and

$$\varsigma=\frac{\hbar\gamma_3}{m_0}\sqrt{\frac{3}{2}},\quad k^+=k_x+ik_y,\quad k^-=k_x-ik_y.$$

Here $P=-(i\hbar/m_0)\langle S|p_x|X\rangle$ is the interband momentum matrix element, and γ_3 is the Luttinger parameter.

If it is applied to quaternary semiconductors in the Pidgeon-Brown treatment, E_g originally is considered as a parameter. Here we use the dependence[3]

$$E_g(x,y,T)=-0.302+6.3\times 10^{-4}(1-2q)T+1.93q-0.81q^2+0.832q^3\quad(\mathrm{eV}), \tag{6}$$

with $q=x+2y$, which takes into account both the compositional bowing and the linear growth of E_g with temperature. Since, without magnetic field, the band gap of $Hg_{1-x-y}Cd_xMn_yTe$ is the same as that of $Hg_{1-x}Cd_xTe$ with $x\to x+2y$, the Luttinger parameters and the interband matrix element for $Hg_{1-x-y}Cd_xMn_yTe$ are chosen to be close to those for $Hg_{1-x}Cd_xTe$, with the effective composition $x_{\mathrm{eff}}=x+2y$: $\Delta=1$ eV, $\gamma_1=3$, $\gamma_2=\gamma_3=0.05$, $\kappa=-1.65$, and $P=8.4\times 10^{-8}$ eV cm.[11] With this parameter set we calculate the Landau levels, and the transition probabilities among them. The exchange parameters as well as the parameters defining the magnetization M, $M=-N_0 y g_{\mathrm{Mn}}\mu_B\langle S_z\rangle$, are assumed to be adjustable. N_0 is here the number of unit cells per volume unit, and two parameters are introduced: $A=N_0\alpha$ stands for the s-d exchange interaction and $B=N_0\beta$ denotes the p-d exchange interaction.

For describing the PL data, one has to take into account that the PL signal is observed in the steady-state regime when all carriers are relaxed after deep band-to-band excitation. Due to thermodynamic considerations, only the lowest Landau levels are filled. In the presence of a magnetic field, the $a(0)$ and $b(0)$ electron states of the conductivity band and the $a(-1)$ and $b(-1)$ heavy-hole states of the valence band determine the energy gap. In the Faraday geometry ($\vec{E}\perp\vec{H}$), the following Γ_8-to-Γ_6 transitions are allowed by symmetry: [11]

σ^+ circular polarization:

$$a_{\Gamma 8}(N)\to a_{\Gamma 6}(N-1),\quad b_{\Gamma 8}(N)\to b_{\Gamma 6}(N-1); \tag{7a}$$

σ^- circular polarization:

$$a_{\Gamma 8}(N)\to a_{\Gamma 6}(N+1),\quad b_{\Gamma 8}(N)\to b_{\Gamma 6}(N+1). \tag{7b}$$

In the Voigt geometry ($\vec{E}||\vec{B}$) we have the following:

linear polarization:

$$a_{\Gamma 8}(N-1)\to b_{\Gamma 6}(N),\quad b_{\Gamma 8}(N+1)\to a_{\Gamma 6}(N). \tag{7c}$$

C. Discussion

The theoretical development described above has been used for a calculation of the resulting matrix elements for the interband transitions. The strongest allowed optical transitions among the eigenstates of Eq. (4) are those proportional to the interband matrix element P. The calculation shows that the transition probabilities critically depend on the exchange interaction. Furthermore, they are much smaller for transitions with participation of heavy-hole Landau levels in σ^+ than in σ^- polarization. From Eq. (7), it follows that in the Faraday geometry one should observe exclusively the $a(-1)\leftrightarrow a(0)$ and $b(-1)\leftrightarrow b(0)$ transitions. In an earlier paper,[3] we showed that for a Mn content up to 2%, the exchange constants A and B are practically invariant, and their ratio $B/A\cong -2$. This result is consistent with that of Bastard

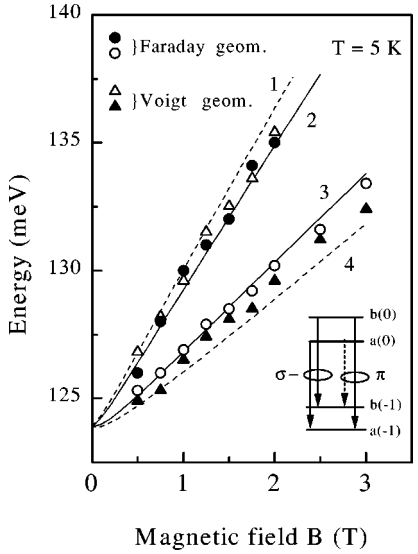

FIG. 3. Spin-splitting Landau levels. Circles correspond to the PL line positions depicted in Fig. 1. The best fit is given as follows: Solid lines—Faraday geometry: (2) $b(0)\rightarrow b(-1)$ transition; (3) $a(0)\rightarrow a(-1)$ transition. Dashed lines—Voigt geometry: (1) $b(0)\rightarrow a(-1)$ transition; (4) transition forbidden by selection rules $a(0)\rightarrow b(-1)$. The inset schematically shows the Landau sublevels involved in the radiative transitions.

et al.,[8] that this ratio is independent of composition and equals -2 for $y\leqslant 0.015$ in dilute $Hg_{1-y}Mn_yTe$ compounds. Therefore, the fitting procedure for the Faraday geometry takes $A=-0.45$ eV as the starting point and the ratio $|B/A|=2$ as constant. Figure 3 depicts the PL data for both Faraday and Voigt geometries. The best fit was achieved with the parameter set $A=-(0.45\pm 0.02)$ eV, $S_0=(2.3\pm 0.1)$, and $T_0=(2\pm 0.2)$ K. The values obtained for S_0 and T_0 indicate that the interaction between intersite Mn^{2+} ions is relatively unimportant. Thus we are able to give a level scheme for the transitions (cf. the inset in Fig. 3). The high-energy component of the PL signature in the presence of a magnetic field is quickly quenched due to the depopulation of the higher Landau level $b(0)$. Such a behavior is consistent with the PL data for the Faraday geometry, where two components can be assigned to $a(-1)\leftrightarrow a(0)$ and $b(-1)\leftrightarrow b(0)$ transitions.

The most unexpected behavior was found, however, for PL in the Voigt geometry. According to the selection rules [Eq. (7c)], only a single transition $a(-1)\leftrightarrow b(0)$ is expected, whereas two components are clearly resolved in the PL spectra. Based on our calculations, the high-energy component is the $a(-1)\leftrightarrow b(0)$ transition. For magnetic fields up to 1.0 T, this is also the dominant feature, since it has the largest transition probability. For increasing magnetic fields its intensity rapidly decreases (cf. Fig. 1). The second PL component practically coincides with the $a(-1)\leftrightarrow a(0)$ transition allowed in the Faraday geometry, but it is also a nearly forbidden $b(-1)\leftrightarrow a(0)$ transition in the Voigt geometry. In both cases, however, one needs to assume that the electrons excited in the Voigt geometry in the $b(0)$ (spin-down) state relax into the $a(0)$ (spin-up) Landau level. This means that, during cooling of the free carriers in the magnetic field, spin-flip transitions between spin-split subbands take place, and this relaxation governs the population of the $a(0)$ subband.

The investigation of the heating of the electron and spin systems in $Cd_{0.232}Hg_{0.768}Te$, which has nearly the same E_g as our samples, has shown another relaxation picture.[12] It has been assumed that three relaxation time constants are relevant: τ_E, the energy relaxation time; τ_R, the radiative lifetime; and τ_S, the spin relaxation time. These time constants were found to be in relation:

$$\tau_S \geqslant \tau_R > \tau_E . \tag{8}$$

τ_S was estimated to be not less than 10^{-6} s at $B=3$ T. The population of the spin subbands in $Cd_{0.232}Hg_{0.768}Te$ did not become an equilibrium one, because the spin relaxation of electrons excited high into the conduction band is switched out at the moment of their recombination. This results in a population of the upper spin subbands which is higher than that expected for equilibrium conditions.

Our PL data for $Hg_{0.769}Cd_{0.224}Mn_{0.007}Te$ convince us that effective spin relaxation (probably caused by the presence of manganese) is quite effective, and produces a stationary population of the $a(0)$ Landau subband. Thus for the semimagnetic material inequality, Eq. (8) must be rewritten

$$\tau_R \geqslant \tau_S > \tau_E , \tag{9}$$

and allows a complete quantitative description of our data obtained in the Faraday and Voigt geometries.

The interpretation given above is also supported by our SdH data. Based on the exchange parameters derived from PL, the Landau-level fan has been calculated for the conduction band. In order to determine the SdH maximum positions one needs to calculate the Fermi energy, which also becomes a function of B. This particular dependence is of great importance for small Landau numbers ($N=0$ and 1). In fact, the function $k_z(E,N,\sigma)$ is sufficient for a determination of all thermodynamic and kinetic properties of semiconductors in quantized magnetic fields. This function is calculated numerically from Eqs. (4) and (5) for each set of N and σ. Taking into account the relation between the chemical potential or Fermi energy E_F and the electron concentration n,[13]

$$N=\frac{eH}{2\pi^2\hbar c}\sum_{N,\sigma}\int_{E_0(N,\sigma)}^{\infty}\left(-\frac{\partial f_0}{\partial E}\right)k_z(E,N,\sigma)dE, \tag{10}$$

where $f_0(E)=[1+\exp[(E-E_F)/k_BT]]^{-1}$ is the Fermi distribution, we determined the $E_F(B)$ dependence for an electron gas of constant density. Figure 4 depicts the Landau-level fan plot for the conduction band and the oscillating Fermi energy calculated for the given situation. At $H\rightarrow\infty$ the Fermi energy tends to the energy $E(N=0)$, and all of the electrons are condensed on the lowest Landau sublevel $[a(0)]$. In strong magnetic fields the condition for SdH oscillations reduces to

$$k_z(E_F,N,\sigma,B)=0, \tag{11}$$

which gives the positions of the magnetoresistance maxima. We solved Eq. (11) considering the left side as a function of the field B. This allowed us to avoid the treatment of the gyromagnetic factor g^* of the carriers in the conduction

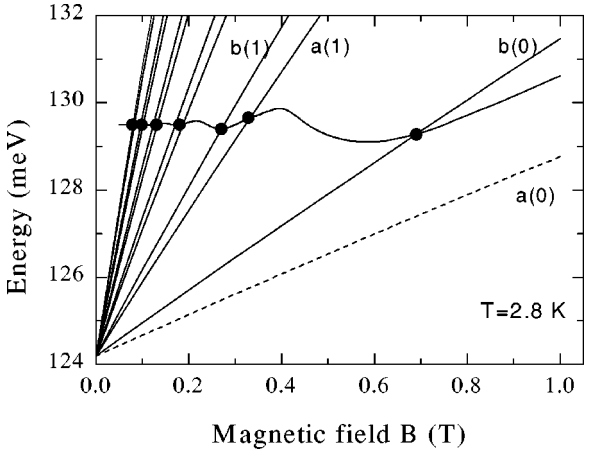

FIG. 4. Landau fan plot for the conduction band calculated using Eq. (4); the other solid curve is the Fermi energy determined using Eq. (10). The theoretically expected SdH maxima are the intersections of the Fermi energy curve with the Landau level (fan) curves. The experimental data of the SdH maxima are given as full circles.

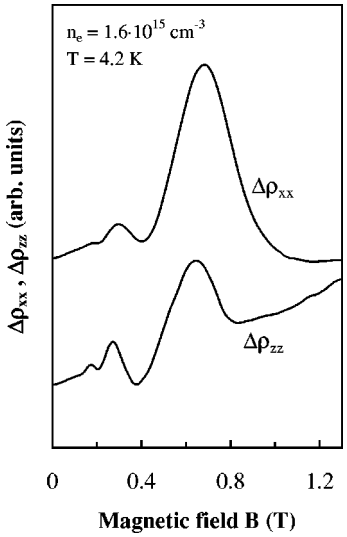

FIG. 5. Oscillating part of the longitudinal ρ_{zz} and transverse ρ_{xx} magnetoresistances in single-crystalline $Hg_{0.769}Cd_{0.224}Mn_{0.007}Te$ at $T=4.2$ K.

band. Now the positions of the SdH maxima for the transverse magnetoresistance ρ_{xx} determined in this way were compared with the data (full points in Fig. 4). This fitting procedure evaluates the exchange parameters to be $A=-(0.47\pm0.03)$ eV and $B=(0.92\pm0.03)$ eV. We believe that the exchange parameters are more accurately determined from the magneto-PL data; they were $A=-(0.45\pm0.02)$ eV and $B=(0.90\pm0.02)$ eV, remarkably close to the values determined from the magnetotransport data.

Finally, the longitudinal and transverse magnetoresistance data were compared to study the effect on the spin relaxation due to exchange interaction. This comparison can usually be accomplished in terms of g^* factor which is immediately calculated from our experiments. The positions of the SdH maxima for ρ_{xx} can be derived:[13–15]

$$H_N^{a,b}=\frac{\hbar c}{e}(\sqrt{2}\pi^2 n)^{2/3}\left\{\sum_{k\geq 0,\mp 2\gamma}^{N}(\sqrt{k}+\sqrt{k\pm 2\gamma})+0.535\sqrt{\frac{k_B T}{\hbar\omega_c}}\right\}^{-2/3}, \tag{12}$$

where m^* is the electron effective mass, $\omega_c=eH/m^*c$ is the cyclotron frequency and the parameter γ is $\gamma=g^*m^*/4m_0$. The $(+)$ and $(-)$ signs correspond to the a and b spin states, respectively. From Eq. (12) it follows that, for constant g^*, increasing temperatures lead to decreasing $H^{a,b}$ values. This change is most pronounced for the first maximum (highest magnetic field maximum). We find a negative value of g^*. In this case the H_0^b peak is the first peak in the $\rho_{xx}(H)$ dependence. Even this peak exhibits a nonmonotonic temperature dependence: approaching lower temperatures it moves towards weaker magnetic fields (see Fig. 2) and opposite for higher temperatures. According to Eq. (12) such a behavior can be understood with the temperature dependence of g^*.

Bearing in mind the selection rules for SdH oscillations[5] it can be stated that H_0^b is forbidden to appear in the longitudinal magnetoresistance ρ_{zz}. Nevertheless Fig. 5 clearly shows even this particular peak for longitudinal configuration. According to Ref. 4, this could be caused by a violation of the selection rules. Note that the selection rules have been derived for the assumption that only an s-like electron wave function is included in the analysis of the spin-orbit coupling. In this approximation the spin-flip transitions between the $a(0)$ to $b(0)$ levels are forbidden. However, if a p-like wave-function contribution to the conduction band is allowed, spin-flip transitions from the $b(0)$ to $a(0)$ states also become probable. The admixture of p-like wave functions increases if the energy gap decreases. Thus this admixture leading to the breaking of the normal selection rules can be considered to be a feature specific to narrow-gap semiconductors. Note that the SdH data, as well as their theoretical description, support the thesis of the relevance of spin-flip transition.

After having discussed the purely experimental evidence for the influence of the exchange interaction on the spin relaxation in $Hg_{1-x-y}Cd_xMn_yTe$, we present a conceptual argument for its reasonableness. Due to the enormous excess energy after excitation in our PL experiment, a large number of scattering steps occurs during the carrier ''cooling.'' A spin flip is very likely to occur at each step. Especially phonon scattering (only partially spin conserving), but also free-carrier spin-spin scattering along with spin-Mn scattering and spin-orbit interaction, may contribute. The main mechanisms of nonequilibrium electron spin relaxation in semiconductors were well reviewed in Refs. 16 and 17. Our experimental results cannot unambiguously distinguish between the possible contributions of the various spin-scattering mechanisms, but the complementary studies of PL and SdH in $Hg_{1-x-y}Cd_xMn_yTe$ indicate that during the relaxation the spin is mostly preserved when a carrier reaches the Fermi energy. The same conclusion can be deduced from the experimental results in nonmagnetic $Hg_{1-x}Cd_xTe$ (Refs. 12 and 18). Following Ref. 19, we assume that for our case of narrow-gap dilute semimagnetics two mechanisms of spin relaxation for the near Fermi-energy electrons are important: Elliott-Yafet spin relaxation,[20,21] and exchange interaction.[19]

Elliott-Yafet relaxation (τ_{EY}) occurs due to the strong influence of the spin-orbit interaction on the band structure. As a result, the p-type wave function mixes with the usual conduction-band state, and spin ceases to be a good quantum number. All scattering mechanisms partly relax the initial spin polarization. The corresponding spin-relaxation rate may be written[19]

$$\frac{1}{\tau_{EY}} \approx \frac{8}{9}\frac{1}{\tau_m}\left(\frac{E_c(k)}{E_g}\right)^2 \eta^2 \frac{2-\eta}{3-\eta}, \tag{13}$$

where $\eta = \Delta/(E_g+\Delta)$; τ_m is the momentum-relaxation time, excluding optical phonon scattering; and Δ is the spin-orbit splitting ($\Delta \sim 1$ eV). The applicability of this equation for the case of narrow-gap semiconductors was discussed in Refs. 19 and 18. If one assumes that τ_m does not depend on the electron energy $E_c(k)$ and takes it to be $\tau_m = 1 \times 10^{-13}$ s,[19] the inverse relaxation time τ_{EY}^{-1} is estimated to be $\tau_{EY}^{-1} = 2.1 \times 10^8$ s^{-1} for electrons in the $b(0)$-related Landau subband at $B = 2$ T.

The s-d-like exchange interaction typical for dilute semimagnetic semiconductors results in a spin-relaxation rate of[19]

$$\frac{1}{\tau_{ex}} = \frac{\chi k_B T k m^*(k)}{\pi \hbar^3 g^2 \mu_B^2}\left[a_c^4\alpha + \frac{1}{4}\left(c_c^4 + \frac{5}{6}b_c^4 + \frac{2b_c^2 c_c^2}{3} + \frac{2\sqrt{2}}{3}b_c^3 c_c\right)\beta^2\right], \tag{14}$$

where a_c describes the s-type component and b_c and c_c denote p-type components in the Bloch function. Their explicit form is given in Refs. 22 and 23. Taking the electron temperature T to be close to that of the lattice (due to the low excitation density, $P \sim 1$ W cm^{-2}), and the exchange parameters determined here from the PL and SdH data (as well as the susceptibility), one can calculate the value $1/\tau_{ex}$ to be $1/\tau_{ex} = 4.1 \times 10^8$ s^{-1}. The numbers obtained show the importance of both the Elliott-Yafet mechanism and the mechanism of exchange interaction, and are to some extent consistent with those derived in Ref. 18. It is not our intention to analyze all the spin-flip mechanisms here, but we can conclude that in dilute semimagnetic n-type $Hg_{1-x-y}Cd_xMn_yTe$ there exist strong matrix elements for spin relaxation. Therefore, the physical picture for the steady-state PL can be drawn: The carrier excited high up into the conduction band quickly loses its excess energy due to inelastic optical-phonon scattering. When it reaches the bottom of the Landau level of the $b(0)$ state, it relaxes into the $a(0)$ state before radiative recombination due to the spin-flip processes proceeds. In the SdH experiments the effect of the exchange and/or Elliot-Yafet mechanism is also relevant, and is made evident by the appearance of the H_0^b peak, which is forbidden for the longitudinal magnetoresistance. It is interesting to note that in $Hg_{1-x-y}Cd_xMn_yTe$ with a wider energy gap than 300 meV, the forbidden peak in SdH measurement is also observed (Ref. 4); however, the PL spectrum (Ref. 3) does not reveal so pronounced a spin-flip dependence as that observed in the samples under consideration.

IV. CONCLUSIONS

We report the results of an experimental study of the magneto-optical and magnetotransport properties of narrow-gap $Hg_{1-x-y}Cd_xMn_yTe$. For both sets of experiments, which were carried out with the same samples, we find direct evidence of the influence of spin-flip transitions. These ''forbidden transitions'' become possible due to peculiarities of both the energy band structure of the narrow-gap semimagnetic semiconductor material and the intermediate free-carrier spin-localized magnetic moment of manganese ion exchange interaction. Thus both the relaxation of photoexcited carriers and their scattering become strongly influenced by such magnetic coupling.

The spin-flip transitions open channels of spin relaxation in comparison with nonmagnetic material with the same E_g (cf. Ref. 12). This process is accompanied by spin-orbit interaction, resulting in a p-type wave-function admixture to the conduction band. In this particular case the spin is no longer a good quantum number, and the usual selection rules are violated. All scattering mechanisms can cause at least a partial relaxation of the initial spin polarization.

The present SdH data display a well-pronounced H_0^b peak which is forbidden in the longitudinal magnetoresistance. Thus we find an indication of the substantial role of spin-dependent scattering mechanisms. Temperature variation shows that, with decreasing temperature, an enhancement of the particular H_0^b peak takes place. Thus evidence of the efficiency of spin-flip transitions under participation of acoustic phonons is given.

We provide a consistent theoretical description of both the PL data and SdH oscillations based on the Pidgeon-Brown model. The parameters, determining the exchange interaction and clustering, are derived by fitting both sets of experimental data. We find the exchange parameters $A = -(0.45 \pm 0.02)$ eV and $B = (0.90 \pm 0.02)$ eV, as well as $T_0 = (2 \pm 0.2)$ K and the ''clustering parameter'' $S_0 = (2.3 \pm 0.1)$.

Our experiments do not allow us to distinguish between the various spin-flip processes possible in narrow-gap semimagnetics. An investigation based on time-resolved spectroscopy will be useful to make this distinction.

ACKNOWLEDGMENTS

The authors are indebted to Dr. S. R. Lavoric for helpful discussions and assistance during manuscript preparation. This work was supported by the Volkswagen Stiftung.

*Electronic address: massel@physik.hu-berlin.de

[1] S. I. Kriven, Yu. I. Mazur, G. G. Tarasov, and N. V. Shevchenko, Fiz. Tverd. Tela (Leningrad) **34**, 955 (1992) [Sov. Phys. Solid State **34**, 510 (1992)].
[2] Yu. I. Mazur, S. I. Kriven, G. G. Tarasov, and N. V. Shevchenko, Semicond. Sci. Technol. **8**, 1187 (1993).
[3] Yu. I. Mazur, G. G. Tarasov, V. Jähnke, J. W. Tomm, and W. Hoerstel, Semicond. Sci. Technol. **11**, 1291 (1996).
[4] S. Takeyama and S. Narita, Solid State Commun. **60**, 285 (1986).
[5] K. Suizu and S. Narita, Phys. Lett. **43A**, 353 (1973).
[6] C. R. Pidgeon and R. N. Brown, Phys. Rev. **146**, 575 (1966).
[7] J. Kossut, in *Diluted Magnetic Semiconductors*, edited by R. K. Willardson and A. C. Beer, Semiconductors and Semimetals Vol. 25, (Academic, New York, 1988), pp. 183–227.
[8] G. Bastard, C. Rigaux, Y. Guldner, J. Mycielski, and A. Mycielski, J. Phys. (Paris) **39**, 87 (1978).
[9] N. V. Brandt and V. V. Moshchalkov, Adv. Phys. **33**, 193 (1984).
[10] W. Leung and L. Liu, Phys. Rev. B **8**, 3811 (1973).
[11] Y. Guldner, C. Rigaux, A. Mycielski, and Y. Couder, Phys. Status Solidi B **82**, 149 (1977).
[12] V. I. Ivanov-Omskii, I. A. Petroff, V. A. Smirnov, J. W. Tomm, and K. H. Herrmann, in *The Physics of Semiconductors* (World Scientific, Singapore, 1990), Vol. 8, p. 1747.
[13] B. M. Askerov, *Electron Transport Phenomena in Semiconductors* (World Scientific, Singapore, 1994).
[14] A. E. Belyaev, O. P. Gorodnichii, Yu. G. Semenov, N. V. Shevchenko, O. A. Bodnaruk, and I. M. Rarenko, Fiz. Tekh. Poloprovodn. **22**, 335 (1988) [Sov. Phys. Semicond. **22**, 205 (1988)].
[15] A. E. Belyaev, N. N. Gavaleshko, S. I. Kriven', Yu. I. Mazur, and N. V. Shevchenko, Fiz. Tekh. Poloprovodn. **24**, 1999 (1990) [Sov. Phys. Semicond. **24**, 1243 (1990)].
[16] G. E. Pikus and A. N. Titkov, in *Optical Orientation*, edited by F. Meier and B. P. Zakharchenya, Modern Problems in Condensed Matter Sciences No. 8 (North-Holland, Amsterdam, 1984), pp. 63–108.
[17] M. I. Dyakonov and V. I. Perel, in *Optical Orientation* (Ref. 16), pp. 11–70.
[18] E. I. Georgitse, V. I. Ivanov-Omskii, V. M. Pogorletskii, and V. A. Smirnov, Semicond. Sci. Technol. **6**, 924 (1991).
[19] H. Krenn, K. Kaltenegger, T. Dietl, T. Spalek, and G. Bauer, Phys. Rev. B **39**, 10 918 (1989).
[20] R. J. Elliott, Phys. Rev. **96**, 266 (1954).
[21] Y. Yafet, Solid State Phys. **14**, 1 (1963).
[22] E. O. Kane, J. Phys. Chem. Solids **1**, 249 (1957).
[23] Yu. I. Mazur, G. G. Tarasov, S. R. Lavoric, J. W. Tomm, H. Kissel, and W. Hoerstel, Phys. Status Solidi B **195**, 595 (1996).